https://doi.org/10.5194/tc-2019-293
Preprint. Discussion started: 9 January 2020
© Author(s) 2020. CC BY 4.0 License.

The Cryosphere Discussions

Seasonal and interannual variability of landfast sea ice in Atka Bay, Weddell Sea, Antarctica

Stefanie Arndt[1], Mario Hoppmann[1], Holger Schmithüsen[1], Alexander D. Fraser[2,3], Marcel Nicolaus[1]

[1]Alfred-Wegener-Institut Helmholtz-Zentrum für Polar- und Meeresforschung, 27570 Bremerhaven, Germany

[2] Institute for Marine and Antarctic Studies, University of Tasmania, Hobart 7001, Tasmania, Australia

[3]Antarctic Climate & Ecosystems Cooperative Research Centre, University of Tasmania, Hobart 7001, Tasmania, Australia

Correspondence to: Stefanie Arndt (stefanie.arndt@awi.de)

Abstract. Landfast sea ice (fast ice), attached to Antarctic coastal and near-coastal elements, is a critical element of the local physical and ecological systems. Through its direct coupling with the atmosphere and ocean, fast ice and its snow cover are also potential indicators of processes related to climate change. However, in-situ fast-ice observations in Antarctica are extremely sparse because of logistical challenges. Since 2010, a monitoring program, which is part of the Antarctic Fast Ice Network (AFIN), has been conducted on the seasonal evolution of fast ice of Atka Bay. The bay is located on the north-eastern edge of Ekström Ice Shelf in the eastern Weddell Sea, close to the German wintering station Neumayer Station III. A number of sampling sites have been regularly revisited between annual ice formation and breakup each year to obtain a continuous record of snow depth, freeboard, sea-ice- and sub-ice platelet layer thickness across the bay.

Here, we present the time series of these measurements over the last nine years. Combining them with observations from the nearby meteorological observatory at Neumayer Station as well as satellite images allows to relate the seasonal and interannual fast-ice cycle to the factors that influence its evolution. On average, the annual consolidated fast-ice thickness at the end of the growth season is about two meters, with a loose platelet layer accumulation of four meters beneath and 0.70 meters snow on top. Results highlight the predominately seasonal character of the fast-ice regime in Atka Bay without a significant trend in any of the observed variables over the nine-year observation period. Also, no changes are evident when comparing with measurements in the 1980s. However, strong easterly winds in the area govern the year-round snow redistribution and also trigger the breakup event in the bay during summer months.

Due to the substantial snow accumulation on the ice, a characteristic feature is frequent negative freeboard, associated flooding of the snow/ice interface and subsequent formation of snow ice. The buoyant platelet-ice layer beneath negates the snow weight to some extent, but snow thermodynamics is identified as the main driver of the energy and mass budgets for the fast-ice cover in Atka Bay.

An enhanced knowledge on the seasonal and interannual variability of the fast-ice properties will improve our understanding of interactions between atmosphere, fast ice, ocean and ice shelves in one of the key regions of Antarctica.

https://doi.org/10.5194/tc-2019-293
Preprint. Discussion started: 9 January 2020
© Author(s) 2020. CC BY 4.0 License.

The Cryosphere Discussions

1 Introduction

The highly dynamic pack ice of the open polar oceans is continuously in motion under the influence of winds and ocean currents (Kwok et al., 2017). In contrast, landfast sea ice (short: fast ice) is attached to the coast or associated geographical features, such as for example a shallow seafloor (especially in Arctic regions) or grounded icebergs, and is therefore immobile (JCOMM Expert Team on Sea Ice, 2015). Fast ice is a predominant and characteristic feature of the Arctic (Dammann et al., 2019; Yu et al., 2014) and Antarctic coasts (Fraser et al., 2012), especially in winter. Its extent may vary between just a few meters and several hundred kilometers from where it is attached to, mostly depending on the local topography and coastline morphology. The main processes for fast-ice formation are either in-situ thermodynamic growth, or dynamic thickening and subsequent attachment of ice floes of any age to the shore (Mahoney et al., 2007b).

In the Arctic, coastal regions that are characterized by an extensive fast-ice cover in winter are for example found in the Chukchi Sea and Beaufort Sea (Druckenmiller et al., 2009; Mahoney et al., 2014; Mahoney et al., 2007a), the Canadian Arctic (Galley et al., 2012), the East Siberian and Laptev Seas (e.g. Selyuzhenok et al., 2017), and the Kara Sea (Olason, 2016). While the fast-ice cover in these regions comes with its own particular impacts on the respective coastal systems, what is common to them is that they have undergone substantial changes in recent decades (Yu et al., 2014). These include a reduction of fast-ice area (Divine et al., 2003), later formation and earlier disappearance (Selyuzhenok et al., 2015) and a reduction of thickness (Polyakov et al., 2003).

Along the Antarctic coastline, the fast-ice belt extends even further from the coast (Fraser et al., 2012; Giles et al., 2008) due to the presence of grounded icebergs in much deeper waters of up to several hundred meters (Massom et al., 2001a). Embayments and grounded icebergs provide additional protection against storms and currents, and are often favorable for the formation of a recurrent and persisting fast-ice cover (Giles et al., 2008). Fast-ice around Antarctica is still usually seasonal rather than perennial, and reaches thicknesses of around 2 meters (Jeffries et al., 1998), although it may attain greater ages and thicknesses in some regions (Massom et al., 2010). It mostly forms and breaks up annually as a response to various environmental conditions, such as heavy storms (Fraser et al., 2012; Heil, 2006). Its immediate response to both local atmospheric conditions but also to lower latitude variability of atmospheric and oceanic circulation patterns via the respective teleconnections (Aoki, 2017; Heil, 2006; Mahoney et al., 2007b), make fast ice a sensitive indicator of climate variability and even climate change (Mahoney et al., 2007a; Murphy et al., 1995). Based on the complexity and significance of fast ice in the Antarctic climate system, there is the urgent need for prognostic Antarctic fast ice in regional models, and later in global climate models, to capture its potential major impacts on the global ocean circulation, as developed for the Artic recently (Lemieux et al., 2016).

Although fast ice only represents a rather small fraction of the overall sea-ice area (Fraser et al., 2012), it may contribute significantly to the overall volume of Antarctic sea ice, especially in spring (Giles et al., 2008). The presence and evolution of fast ice is often associated with the formation and persistence of coastal polynyas, regions of particular high sea-ice production (Fraser et al., 2019; Massom et al., 2001a; Tamura et al., 2016; Tamura et al., 2012) and Antarctic Bottom Water formation

https://doi.org/10.5194/tc-2019-293
Preprint. Discussion started: 9 January 2020
© Author(s) 2020. CC BY 4.0 License.


(Tamura et al., 2012; Williams et al., 2008). Also, it forms an important boundary between the Antarctic ice sheet and the pack ice/ocean, for example prolonging the residence times of icebergs (Massom et al., 2003), mechanically stabilizing floating glacier tongues and ice shelves, and delaying their calving (Massom et al., 2010; Massom et al., 2018). Therefore, one particularly interesting aspect of Antarctic fast ice is its interaction with nearby ice shelves, floating seaward extensions of the continental ice sheet that are present along nearly half of Antarctica's coastline. Under specific oceanographic conditions, supercooled Ice Shelf Water favors the formation of floating ice crystals deep in the water column (Foldvik, 1977). These crystals may be advected out of an ice-shelf cavity and rise to the surface (Hoppmann et al., 2015b). They are eventually trapped under a nearby fast-ice cover and may accumulate in a layer reaching several meters in thickness (Gough et al., 2012). This sub-ice platelet layer has profound consequences for the local sea ice system, forming an entirely unique habitat. Thermodynamic growth of the overlying solid fast ice into this layer leads to subsequent consolidation, and the resulting incorporated platelet ice may contribute significantly to the local fast-ice mass and energy budgets. This phenomenon has been documented at various locations around Antarctica (Langhorne et al., 2015), and where present, is a defining feature of the local coastal system.

The effects of fast ice on the exchange processes between ocean and atmosphere are further amplified by the accumulation of snow, as it forms a thick layer in large parts of the Antarctic sea ice (Massom et al., 2001b). However, the snow cover has very opposing effects on the energy and mass budgets of sea ice in the region. Due to its low thermal conductivity, snow acts first as a barrier to heat transfer from sea ice to the atmosphere and effectively reduces ice growth at the bottom (Eicken et al., 1995). On the other hand, snow contributes significantly to sea-ice thickening at the surface through two distinct seasonal processes, snow-ice and superimposed ice formation. In winter/spring, the heavy snow load leads to the depression of the sea-ice surface below water level causing flooding of the snow/ice interface. The subsequent refreezing of the snow/water mixture forms a salty layer of so-called snow-ice (e.g. Eicken et al., 1994; Jeffries et al., 1998; 2001). In contrast, in summer, internal snow melt leads to melt water percolating to the snow/ice interface where it refreezes and forms fresh superimposed ice (Haas, 2001; Haas et al., 2001; Kawamura et al., 2004). Both processes contribute significantly to sea-ice growth from the top and thus to the overall sea-ice mass budget in the Southern Ocean.

Last but not least, fast ice plays an important role for the ice-associated ecosystem in the Southern Ocean, as it provides a stable habitat for microorganisms (e.g. Günther and Dieckmann, 1999) and serves as a breeding ground for, e.g., Weddell seals and Emperor penguins (Massom et al., 2009).

Fast ice and its properties as described above have been studied around Antarctica for a long time period, especially related to logistical work at the summer and overwintering bases close to the coast of the continent. In order to commonly coordinate and facilitate this research, and thus establish an international network of fast-ice monitoring stations around the Antarctic coastline, the international Antarctic Fast Ice Network (AFIN) was initiated during the International Polar Year (IPY) 2007/2008 (Heil et al., 2011). Active international partners are, e.g., Australia working at Davis Station on the eastern rim of Prydz Bay in East Antarctica (Heil, 2006), New Zealand in McMurdo Sound at Scott Base in the Ross Sea (Smith et al., 2001), and Norway at the fast ice in front of Fimbul ice shelf at Troll Station (Heil et al., 2011) and Germany in Atka Bay at Neumayer

https://doi.org/10.5194/tc-2019-293
Preprint. Discussion started: 9 January 2020
© Author(s) 2020. CC BY 4.0 License.


Station III (Hoppmann et al., 2013), both in the vicinity of Dronning Maud Land. The regular monitoring program at Neumayer Station III related to AFIN started in 2010 in order to fill the knowledge gap in the Weddell Sea sector.

Here we present a decade of annual in-situ fast-ice observations in Atka Bay, which is the longest and most continuous time series within AFIN today. The main dataset is a semi-continuous record of fast-ice thickness, snow depth, freeboard, and sub-ice platelet layer thickness that was collected by a number of overwintering teams between 2010 and 2018. In addition to determining the spatio-temporal variability of the fast-ice cover, we co-analyze this data with meteorological and oceanographic observations in order to determine how snow and platelet ice influence the local fast-ice mass budget. In doing so, we aim to improve our understanding of the interaction between atmosphere, fast ice, ocean and ice shelves in one of the key regions in Antarctica.

2 Study site and measurements

2.1 Study site: Atka Bay

The main study area of this paper is Atka Bay, an 18 km-by-25 km embayment in front of the Ekström Ice Shelf located on the coast of Dronning Maud Land in the eastern Weddell Sea, Antarctica, at 70° 35'S/ 7°35'W (Figure 1). Atka Bay is flanked towards the east, south and west by a floating ice shelf rising up to 20 meters above sea level, and is seasonally sea-ice covered. The water depth ranges between 100 and 500 m with a steep canyon of 275 m in the central bay (Kipfstuhl, 1991). Since the 1980s, when the first German research station Georg-von-Neumayer Station was established in the region, measurements have been carried out in the bay. Today's German research station Neumayer Station III is located at a distance of about 8 km from the bay, where drifting snow regularly forms natural ramps from sea ice to the ice shelf surface. Investigations of the interactions between shelf ice, sea ice and ocean in the bay and its surroundings have been carried out by, e.g., Kipfstuhl (1991); and Nicolaus and Grosfeld (2004), as well as recently by Hoppmann et al. (2015a); and Hoppmann et al. (2015b).

https://doi.org/10.5194/tc-2019-293
Preprint. Discussion started: 9 January 2020
© Author(s) 2020. CC BY 4.0 License.

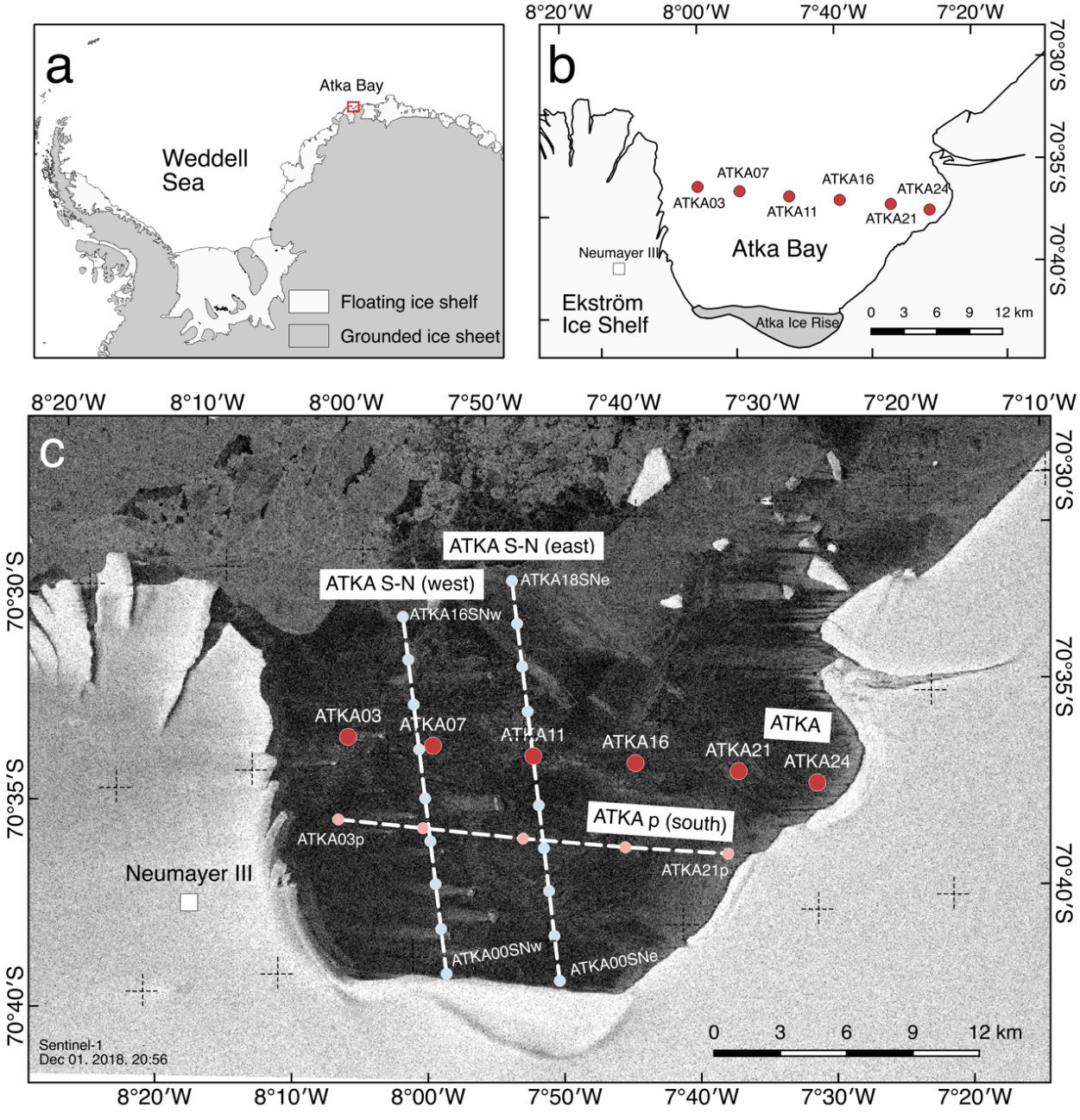

Figure 1. Overview of the study site and its surrounding. (a) Atka Bay (red marker) is located at the edge of the northeastern Weddell Sea. (b) Close-up of map (a) to focus on the study site of Atka Bay. The sampling sites of the standard transect (ATKA) are marked with red circles. (c) Enlargement of (b) showing in addition to the standard transect (red circles) the parallel transect in the south (ATKA p; light red circles) from ATKA03p to ATKA21p in same distances to the western shelf-

https://doi.org/10.5194/tc-2019-293
Preprint. Discussion started: 9 January 2020
© Author(s) 2020. CC BY 4.0 License.


ice edge as the standard transect as well the eastern and western perpendicular transects ATKA S-N (east) from ATKA00SNe to ATKA18SNe and ATKA S-N (west) from ATKA00SNw to ATKA16SNw, each with a distance of 2 kilometers between the sampling sites (light blue circles), all sampled additionally in November/December 2018. In the background a Sentinel-1 images is shown, taken on December 01, 2018.

2.2 Sea-ice conditions

Atka Bay is seasonally covered with sea ice, attached to the shelf forming fast ice. Following the method of fast ice time series retrieval detailed in Fraser et al. (2019), we obtained year-round estimates of fast ice extent in Atka Bay from MODIS visible and thermal infrared satellite imagery. Hence, the fast ice extent time series presented here is a) produced at a 1 km spatial and 15 day temporal resolution, from 15-day MODIS cloud-free composite images (following Fraser et al., 2010) and edge-detected non-cloud-filtered composite images; b) spans the time period from March 2000 to March 2018, c) is semi-automated in the sense that the fast ice edge is automatically delineated during times of high contrast to offshore pack ice/open water, and manually delineated at other times.

Accordingly, the initial ice formation in the bay has started in March in recent years (Figure 2), with persistent easterly winds forcing increased dynamic sea-ice growth towards the western shelf-ice edge of the bay. Once the bay is usually completely covered by fast ice at the end of April (Figure 2), further thermodynamic growth takes place. In the following summer, the ice does not melt in situ, but breaks up and drifts out of the bay once the conditions are sufficiently unstable. Stabilization and breakout of the ice-covered bay is mainly driven by the presence/absence of pack ice offshore Atka Bay associated with changing ocean currents, winds as well as stationary and passing icebergs. Thus, fast-ice break-up in the bay starts usually in December/January after the pack ice in front of the fast ice has retreated (Figure 2).

During our study period from 2010/2011 to 2018/19, there are two exceptions: In September 2012, a large iceberg (B15G) grounded in front of Atka Bay sheltering the fast ice in the bay and consequently preventing sea-ice break-up in the following summer (Hoppmann et al., 2015b) causing second-year fast ice in the bay in 2013. A year later, in August 2013, the iceberg dislodged itself drifting westwards following the Antarctic coastal current. Parts of the iceberg stayed in the vicinity of the bay causing the bay to be blocked a second time two years later, and therefore preventing sea-ice break-up in austral summer 2014/2015 again. The iceberg fragments also drifted out of the vicinity of Atka Bay in the course of the following year, causing the bay to be ice-free in summer afterwards.

https://doi.org/10.5194/tc-2019-293
Preprint. Discussion started: 9 January 2020
© Author(s) 2020. CC BY 4.0 License.

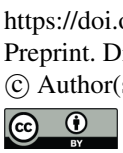

The Cryosphere Discussions
Open Access
EGU

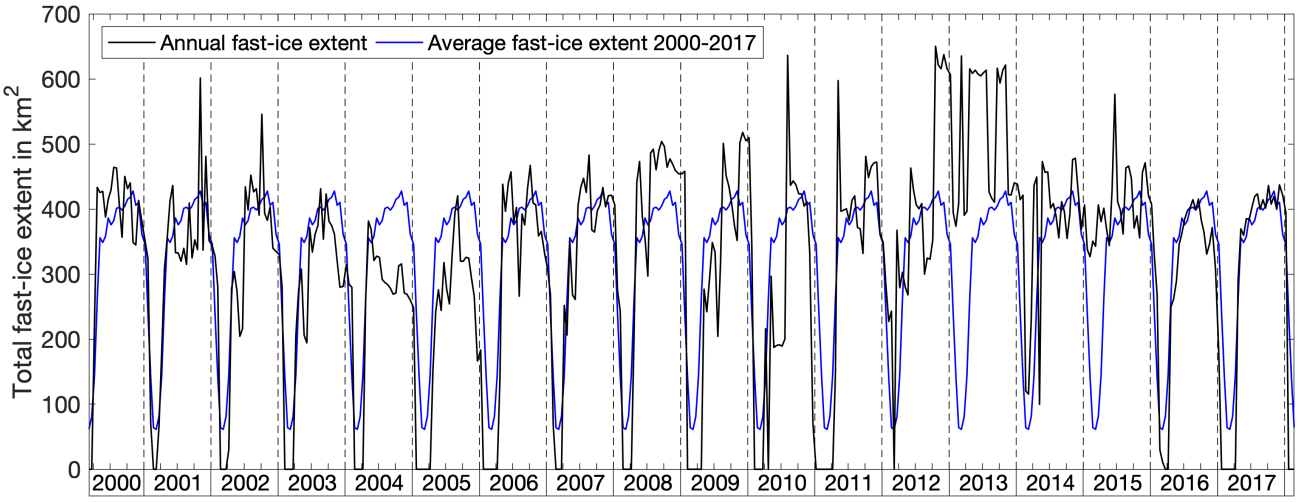

Figure 2: Time-series (black) of fast-ice extent in Atka Bay between 8° 12'W and 7° 24'W derived from MODIS data between early 2000 to early 2018. The blue line shows the annual mean extent repeated over the same time period.

2.3 Sea-ice measurements across Atka Bay

Since 2010, the AFIN monitoring protocol has been implemented to study the seasonal evolution of fast ice along a 24-km long west-east transect in Atka Bay (standard transect, red circles in Figure 1). Here, six sampling sites have been regularly revisited between annual ice formation and breakup each year to obtain a continuous record of snow depth, freeboard, sea-ice- and sub-ice platelet layer thickness across the bay (Arndt et al., 2019). Sampling sites on the standard transect are referred to in this paper as ATKAxx, where xx represents the distance in kilometres to the ice shelf edge in the west.

Generally, measurements along that standard transect are carried out once a month by the wintering team mainly between June and January, when safe access to the ice is secured. At each sampling site, up to five measurements are taken in an undisturbed area, one as the centre measurement and one at a distance of approx. 5 meter in each direction. However, due to time restrictions or very thick snow, sea-ice and platelet ice layers in years of second-year ice in the bay (2012/2013, 2014/2015), measurement frequencies per sampling site are partly reduced to the centre measurement only. For this paper, all measurements along the standard transect from 2010/2011 to 2018/2019 are included, however, the measurements will proceed beyond that time period in the future.

In November and December 2018, additional measurements in both parallel and perpendicular transect lines to the standard transect have been performed (Figure 1). Sampling sites on parallel transects are referred to in this paper as ATKAxxp, where xx represents the distance in kilometres to the ice shelf edge in the west. Along the perpendicular western (w) and eastern (e) transects from south to north, sampling sites are referred to in this paper as ATKAyySNw and ATKAyySNe, where yy represents the distance in kilometres to the ice shelf edge in the south.

https://doi.org/10.5194/tc-2019-293
Preprint. Discussion started: 9 January 2020
© Author(s) 2020. CC BY 4.0 License.


Sea-ice and platelet-ice thickness as well as freeboard are measured with a modified thickness tape. An additional metal bar at the bottom of the thickness tape allows the penetration of the strongly buoyant platelet ice. The underside of the platelet ice is then determined by gently pulling up the tape and attempting to feel the first resistance to the metal bar. Snow depth was measured by using ruler sticks. Freeboard is defined as the distance between snow/ice interface and sea-water level, while the snow/ice interface above (below) sea-water level is referred to as positive (negative) freeboard.

We also calculate the freeboard, F, assuming a hydrostatic equilibrium for floating snow-covered sea ice with an additional buoyancy of the ice platelets below, using Archimedes' law:

$$F = \frac{I\cdot(\rho_I-\rho_W)+S\cdot\rho_S+P\cdot(\rho_P-\rho_W)}{\rho_W}, \qquad \text{(Eq. 1)}$$

where the indices I refers to sea ice, S to snow, P to platelet ice, and W to water, for which constant typical densities of ρ_I = 1032.3 kg m^{-3}, ρ_S = 330 kg m^{-3} and ρ_W = 925 kg m^{-3} are assumed in this study. For platelet ice, a constant ice-volume fraction of β = 0.25, as suggested by Hoppmann et al. (2015b), we use in this paper.

The described bore-hole measurements are occasionally complemented by additional total sea-ice thickness measurements (sea-ice thickness plus snow depth) with a ground-based electromagnetic induction instrument (e.g. Hunkeler et al., 2016) as well as autonomous ice tethered systems, as, e.g. Ice Mass balance or Snow Buoys (Grosfeld et al., 2015; Hoppmann et al., 2015a). However, this paper focusses on the bore-hole measurements only, as the additional observations address scientific questions beyond the scope of this paper.

2.4 Meteorological conditions and observations at Neumayer Station III

At the meteorological observatory of the nearby wintering station Neumayer III, atmospheric conditions have been recorded since 1981 (König-Langlo and Loose, 2007), covering the sea-ice study period from 2010/2011 until today (Schmithüsen et al., 2019). In addition, automatic weather stations (AWS) were temporarily installed on the ice to record the meteorological conditions (Hoppmann et al., 2015a). The comparison of wind speed and direction at 10 meters above sea level between measurements at the meteorological observatory at Neumayer Station III and the AWS on the ice shows a good agreement (Hoppmann et al., 2015a; Hoppmann et al., 2013). Therefore, we utilize in this paper the data of the meteorological observatory at Neumayer Station III to investigate the links between sea-ice conditions and atmospheric circulation patterns.

Generally, in the vicinity of Neumayer Station III, the weather is strongly influenced by cyclonic activities which are dominated by easterly moving cyclones north of the station leading to the prevailing persistent and strong easterly winds showing a seasonal cycle with strongest winds during winter time (Figure 3). The second mode in in the wind distribution in westerly direction (270°) is associated with super geostrophic flows resulting from a high-pressure ridge north of Neumayer Station (König-Langlo and Loose, 2007). These strong winds lead to frequently drifting and blowing snow. Here, we expect snow transport for 10-m wind velocities exceeding 7.7 m/s for dry snow and exceeding 9.9 m/s for wet snow (Li and Pomeroy, 1997).

https://doi.org/10.5194/tc-2019-293
Preprint. Discussion started: 9 January 2020
© Author(s) 2020. CC BY 4.0 License.

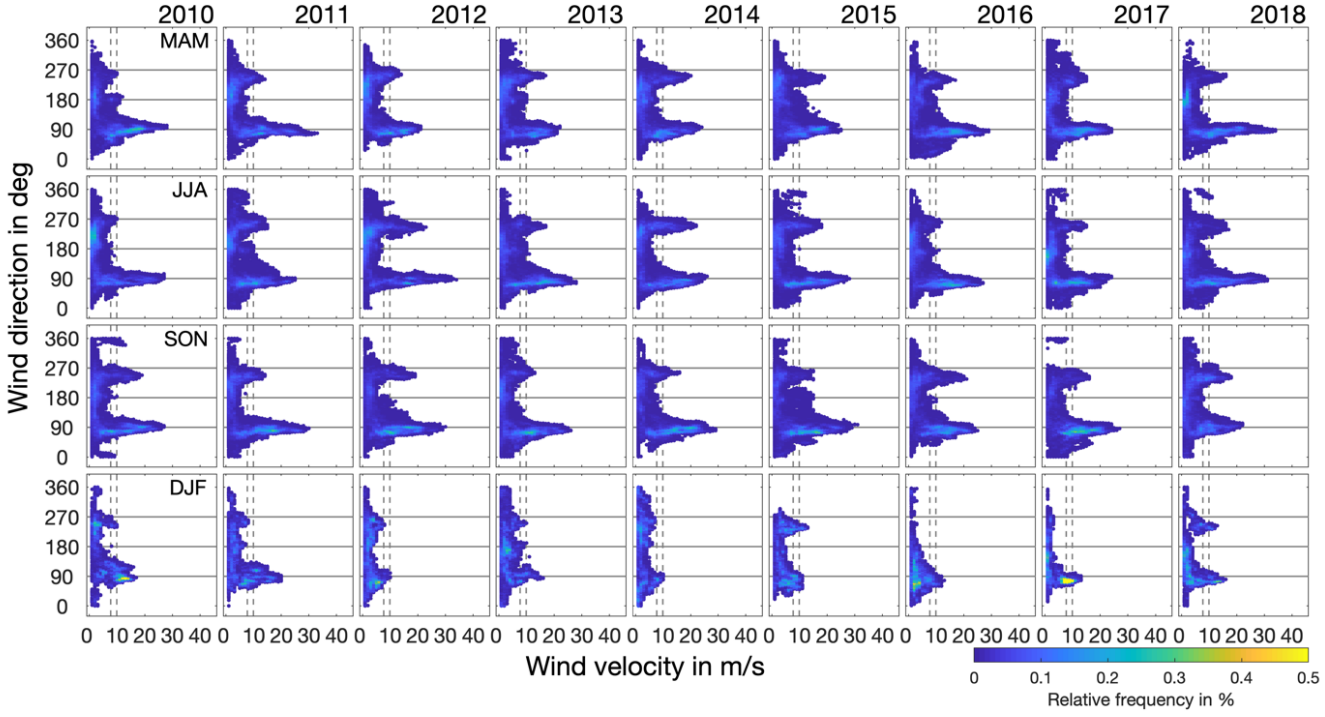

Figure 3: Distribution of wind velocities related to wind directions separated for austral fall (March, April, May; MAM), winter (June, July, August; JJA), spring (September, October, November; SON), and summer (December, January, February; DJF) for the study period from 2010 to 2018. Colors indicate the relative frequency of each shown value pair. Dashed vertical lines denote thresholds for 10-m wind speeds for snow transport of dry (7.7 m/s) and wet snow (9.9 m/s) (Li and Pomeroy, 1997).

3 Results

3.1 Nine-year record of snow, sea-ice and platelet-ice thickness and freeboard along a 24-km W-E transect

Figure 4 summarizes all conducted measurements of snow depth, sea-ice and platelet ice thickness on the standard transect from bore-hole measurements for each ATKA sampling site for the study period from 2010 to 2018. In the seven months, usually from May/June to December, when sea ice conditions allowed safe access, about eight series of measurements were taken along the standard transect crossing Atka Bay, i.e. every three to four weeks.

Analyzing the average annual maximum values of the investigated parameters (Table 1) for years of seasonal fast ice only (excluding 2013 and 2015) and neglecting local iceberg disturbances (ATKA07 in 2017), highest snow accumulation of 0.89 ± 0.36 m was measured at ATKA07, while the smallest by far was measured at ATKA24 at the easternmost sampling site, with only 0.28 ± 0.19 m. Averaging the snow accumulation over the entire bay, the lowest snow accumulation of 0.51 ± 0.30

https://doi.org/10.5194/tc-2019-293
Preprint. Discussion started: 9 January 2020
© Author(s) 2020. CC BY 4.0 License.


m was observed in 2016. In contrast, 2011 was the year with the most snow and an average snow depth of 0.85 ± 0.20 m across the bay. The mean thermodynamically grown seasonal fast-ice thickness over the entire bay during the observation period is varying between 1.74 ± 0.31 m (ATKA21) and 2.58 ± 1.28 m (ATKA07) with a mean value of 1.99 ± 0.63 m. The underlying seasonal platelet-ice layer has accumulated to an average thickness of 3.91 meters each year, which, however, shows a strong gradient in the average annual maximum values (Table 1) from 4.62 ± 0.67 m at ATKA07 in the west of the bay to 2.82 ± 1.20 m at ATKA24 in the east.

In those years, when the fast ice in Atka Bay became second-year ice due to blocking icebergs in front of the bay, an average of additional 0.88 ± 0.43 m of snow accumulated on the seasonal snow cover over the entire bay in 2013 and 0.74 ± 0.27 m in 2015. The average fast-ice thickness across the bay increased by another 1.21 ± 0.42 m in 2013, while it even increased by an additional 2.79 m ± 1.48 m in 2015. The underlying second-year platelet-ice thickness added an additional accumulation of on average 5.13 m ± 1.43 m in 2013 and 4.11 m ± 1.86 m in 2015, with highest additional accumulation at ATKA11 of 6.82 m and 6.44 m, respectively.

https://doi.org/10.5194/tc-2019-293
Preprint. Discussion started: 9 January 2020
© Author(s) 2020. CC BY 4.0 License.

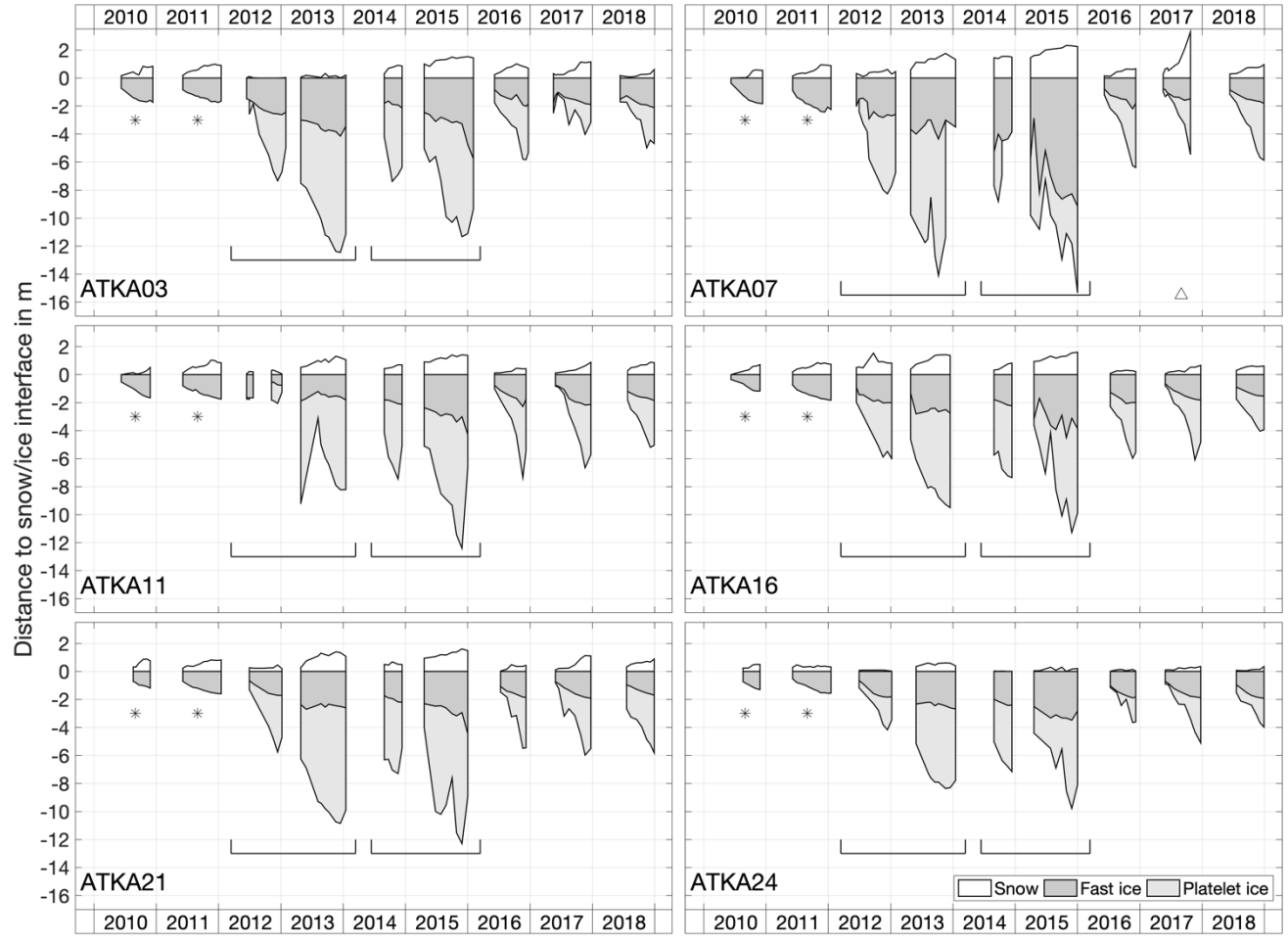

Figure 4: Time series of snow, fast-ice and platelet ice thickness from bore-hole measurements along the standard transect for each ATKA sampling site (Figure 1) for the time period from 2010 to 2018. Note: In 2010 and 2011 the platelet-ice thickness was not measured (*). In 2012/2013 and 2014/2015 Atka Bay was blocked by icebergs, so the fast ice did not break up and turned into second-year ice (⌙). In 2017, a small iceberg in the vicinity of ATKA07 has strongly influenced the snow measurements (△). Reference depth of 0 meters is the snow/ice interface.

The evolution of the freeboard along the standard transect in the study period from 2010 to 2018 is illustrated in Figure 5. Taking all conducted freeboard measurements from seasonal fast ice into account, 55% reveal negative data, i.e. flooding can be assumed, with an average negative freeboard of -0.10 ± 0.08 m. In contrast, considering freeboard measurements from second-year ice only, 38% of the data indicate a negative freeboard with an average height of -0.22 ± 0.15 m. Analyzing the average annual maximum of the negative freeboard values (Table 1) for years of seasonal fast ice only and neglecting local iceberg disturbances (ATKA07 in 2017), there is no distinct gradient across Atka Bay, but higher averaged negative freeboard

https://doi.org/10.5194/tc-2019-293
Preprint. Discussion started: 9 January 2020
© Author(s) 2020. CC BY 4.0 License.

values (-0.07 to -0.08 m) are recorded both in the west (ATKA03) and in the east (ATKA16 and ATKA21), whereas the lowest average negative freeboard of -0.01 ± 0.08 m was measured at ATKA07. According to Equation EQ_FB, 89% of the calculated freeboard values are smaller than the measured values. The difference between measured and calculated freeboard values ranges from -0.19 to 0.54 m with an average of 0.08 ± 0.10 m (towards higher measured value). Neglecting the underlying buoyant platelet-ice layer in the calculation reduces the freeboard by 0.09 ± 0.06 m, whereas neglecting the snow layer on top of the ice increases the freeboard by 0.20 ± 0.17 m (Figure 5).

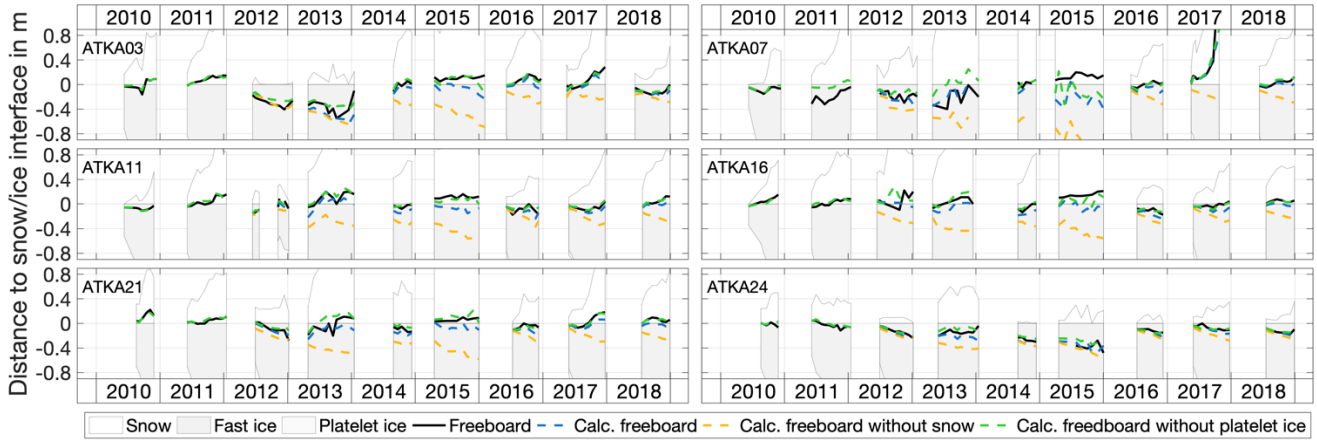

Figure 5: Close-up of Figure 4 around the snow/ice interface in order to display the freeboard as measured in the field (black solid line) and as calculated according to Equation 1 including snow and platelet-ice thickness (blue dashed line), neglecting the snow cover (dashed yellow line) and platelet ice (dashed green line), respectively. For better illustration, all freeboard values are drawn as it is measured in the field, i.e. if the water level is above the snow/ice interface, the freeboard is marked accordingly. Note, however, that the value of the freeboard above the snow/ice interface is negative and vice versa. Reference depth of 0 meters is the snow/ice interface.

Table 1: Average annual maximum of snow depth, sea-ice and loose platelet ice thickness, and freeboard (negative equals potential flooding) on the standard transect from bore-hole measurements for each ATKA sampling site (Figure 1) for the time period from 2010 to 2018, excluding years of second-year ice due to blocking of the bay (i.e. 2013 and 2015). [1]At ATKA11 all measurements of the year 2012 are also neglected as the ice has temporarily broken up again. [2]At ATKA07 the snow measurements of the year 2017 are also neglected as a small iceberg has strongly influenced the accumulation rates. Standard deviations are given in brackets.

	ATKA03	ATKA07	ATKA11	ATKA16	ATKA21	ATKA24
Snow depth in m	0.81 (0.35)	0.89 (0.36)[2]	0.74 (0.23)[1]	0.79 (0.37)	0.77 (0.24)	0.28 (0.19)

https://doi.org/10.5194/tc-2019-293
Preprint. Discussion started: 9 January 2020
© Author(s) 2020. CC BY 4.0 License.

The Cryosphere Discussions

Ice thickness in m	2.04 (0.31)	2.58 (1.28)	1.97 (0.25)[1]	1.81 (0.36)	1.74 (0.31)	1.83 (0.35)
Platelet ice thickness in m	3.88 (1.31)	4.62 (0.47)	4.59 (0.83)[1]	3.99 (0.94)	4.21 (0.54)	2.82 (1.20)
Freeboard in m	-0.08 (0.14)	-0.01(0.08)[2]	-0.05(0.08)[1]	-0.07 (0.09)	-0.08 (0.10)	-0.05 (0.09)

3.2 Seasonal snow, sea-ice and platelet ice growth rates

Figure 6 summarizes the seasonal sea-ice growth as well as snow and platelet-ice accumulation rates separated for austral fall (March, April, May; MAM), winter (June, July, August; JJA), spring (September, October, November; SON), and summer (December, January, February; DJF) for each ATKA sampling point for the study period from 2010 to 2018.

Considering the average monthly snow accumulation rates, a slight increase from fall (from 0.04 to 0.09 m per month) to spring (0.09 to 0.11 m per month) becomes apparent, if excluding the eastern sampling sites at ATKA21 and ATKA24. Latter sampling sites show highest monthly averaged accumulation rates during austral fall (0.11 and 0.08 m per month), which subsequently decrease to 0.10 and 0.02 m per month, respectively. In contrast, a clear snow loss with a maximum monthly average of up to 0.03 ± 0.12 m at ATKA11 and a maximum snow loss rate of 0.21 m per month at ATKA07 (80^{th} percentile), can be seen mostly during summer months. Also, the seasonal evolution of the platelet ice layer shows a similar pattern: between austral autumn and spring an increasing average monthly accumulation rate of up to 0.82 ± 0.30 m at ATKA11 is observed. Excluding ATKA07, afterwards an average monthly platelet-ice loss of 0.85 m is calculated for summer, with a maximum platelet-ice loss rate of 6.25 m per month at ATKA11 (80^{th} percentile). In contrast, ATKA07 also reveals an increase in platelet-ice accumulation during the summer months with an average monthly rate of 0.67 ± 1.20 m. With regard to the growth rates of fast ice in Atka Bay, a contrasting but expected seasonal development is observed: The highest average monthly fast-ice growth rates of up to approx. 1 m per month (80^{th} percentile) are measured in autumn, which decrease in the following month until spring, and therefore describes typical thermodynamic sea-ice growth. In the following summer months, average monthly sea-ice thickness rates increased again to values between 0.07 m (ATKA07) and 0.24 m (ATKA21), except for ATKA24, where even sea-ice melt dominates with an average monthly melt rate of 0.05 ± 0.22 m and a maximum monthly sea-ice melt rate of 0.58 m.

https://doi.org/10.5194/tc-2019-293
Preprint. Discussion started: 9 January 2020
© Author(s) 2020. CC BY 4.0 License.

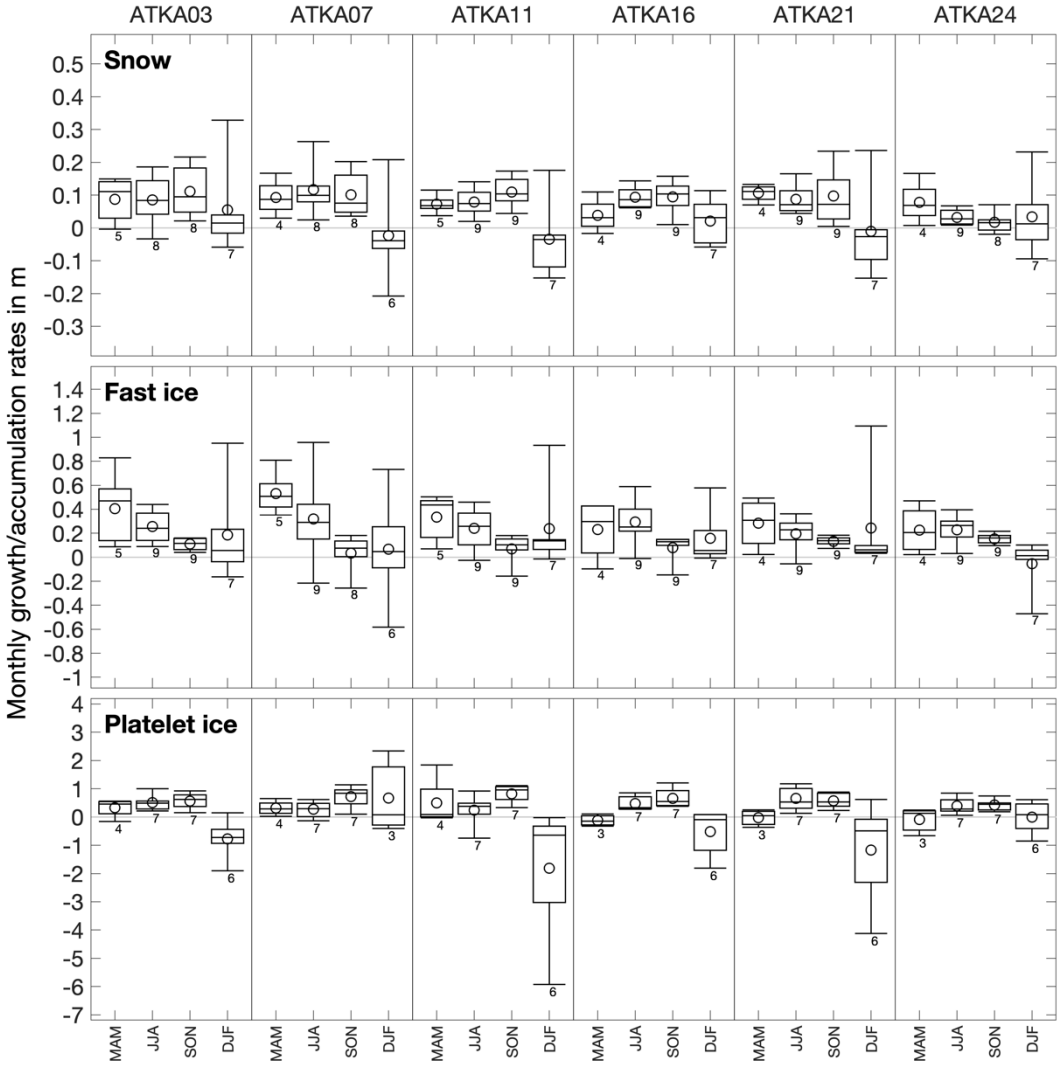

Figure 6: Seasonal sea-ice growth and snow and platelet-ice accumulation rates separated for austral fall (March, April, May; MAM), winter (June, July, August; JJA), spring (September, October, November; SON), and summer (December, January, February; DJF) for each ATKA sampling point for the study period from 2010 to 2018. Boxes are the first and third quartiles; whiskers the 20th and 80th percentile. Circles indicate the mean, vertical lines in the boxes the median. Numbers below the whiskers indicate the respective sampling size, i.e. the number of included years, with a maximum of nine.

3.3 Spatial variability of snow, fast-ice and platelet-ice thickness

In order to describe the spatial variability of snow, fast-ice and platelet-ice thickness in west-to-east as well as in south-to-north direction across Atka Bay, additional parallel and perpendicular transects to the standard transect have been sampled in

https://doi.org/10.5194/tc-2019-293
Preprint. Discussion started: 9 January 2020
© Author(s) 2020. CC BY 4.0 License.

November/December 2018 (Figure 7). Considering the thermodynamically grown ice only, the fast-ice thickness over the bay in south-north and west-east direction is rather constant with an average sea-ice thickness of 1.68 ± 0.21 m. In contrast, neglecting the measurements in iceberg-affected areas, snow accumulation data show higher depth in the south and in the center of the bay with values of up to 1.00 ± 0.04 m, while this decrease significantly towards the eastern shelf-ice edge and northern fast-ice edge to 0.08 ± 0.01 m and 0.28 ± 0.09 m, respectively. Also, the platelet-ice accumulation beneath the fast ice shows a large spatial variability. While all measurements on the standard transect reveal lowest platelet ice accumulation in the east of the bay at ATKA24 (see Section 3.1), on the parallel transect in the south a maximum in the platelet ice accumulation of 7.18 ± 0.26 m at the easternmost sampling point (ATKA21p) is observed. For the perpendicular transects in south-to-north direction, a significant decreasing gradient in platelet-ice thickness from the shelf-ice edge towards the sea-ice edge is evident. Here on the western south-north transect there has been a decrease from 6.62 ± 0.25 m to 2.33 ± 0.08 m, whereas for the eastern transect this is even more apparent with a decrease from 9.17 ± 0.11 m to 1.88 ± 0.20 m.

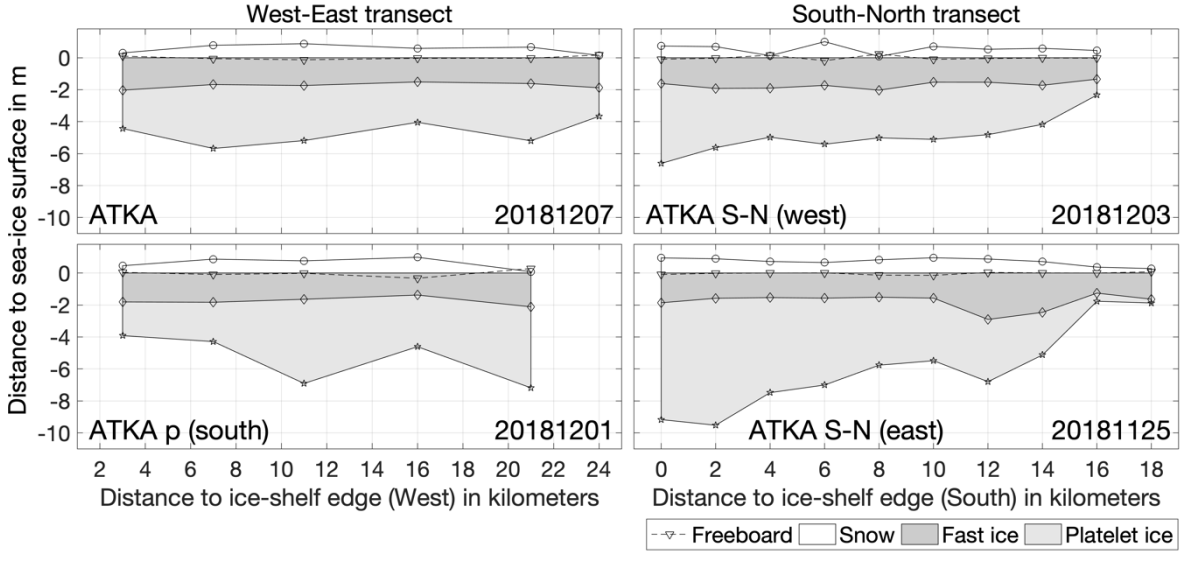

Figure 7: Overview on transect measurements on the standard transect from west to east (upper left), the parallel one (lower left), the western perpendicular transect from south to north (upper right) and the respective parallel one in to the east (lower right) measuring freeboard, snow depth, fast-ice and platelet-ice thickness across Atka Bay. All measurements were conducted between November 25, 2018 and December 07, 2018. For the parallel west-east transect (December 01, 2018), the platelet-ice accumulation is influenced by an iceberg nearby (see Figure 1 c). Also, for the western north-south transect (December 03, 2018), snow measurements are influenced by several small icebergs in the vicinity between kilometers 4 and 8 (see Figure 1 c).

https://doi.org/10.5194/tc-2019-293
Preprint. Discussion started: 9 January 2020
© Author(s) 2020. CC BY 4.0 License.


4 Discussion

4.1 Seasonal and interannual variability of snow, sea-ice and platelet-ice thickness across Atka Bay

The fast-ice regime in Atka Bay is primarily seasonal and only remains in the bay if the breakout is prevented by icebergs in front of it. It has been shown that not only the size of the icebergs plays a role here, but above all the location and the associated influence on altered atmospheric and oceanic circulation patterns. Thus, while in 2013 a 17km-by-10km big iceberg (B15G) blocked the entire bay, in 2015, small icebergs in front of the bay were sufficient to ensure that the sea ice in the bay did not break out, but became perennial.

Considering first of all seasonal sea ice only, the presented measurements along that standard transect across Atka Bay indicate a clear seasonal cycle in all investigated variables, i.e. snow depth, fast-ice and platelet-ice thickness: The initial sea-ice formation in Atka Bay starts in March and proceeds towards a completely fast-ice-covered bay at the end of April. The continuous thermodynamic sea-ice growth proceeds with decreasing growth rate through fall and winter until the thickening snow cover completely isolates heat fluxes between the upper ocean and the atmosphere preventing further thermodynamic growth. However, the fast-ice thickness further increases in spring and shows a significant increase in growth rates during austral summer months which might be associated with consolidation processes of the platelet-ice layer below, i.e. bottom growth as reported by Hoppmann et al. (2015b). Furthermore, the platelet ice is an efficient buffer between the fast ice and the incoming warmer water in summer (Eicken and Lange, 1989), so that no noticeable bottom melt of the fast ice is detected.

Destabilization of the fast ice and the platelet-ice layer below in summer is mainly driven by the presence/absence of pack ice offshore Atka Bay. Thus, the initial breakup and subsequent retreat of the pack ice in front of the bay allow for locally increasing ocean currents beneath the fast ice and the inflow of warm Antarctic Surface Water from the east (Hoppmann et al., 2015a; Hattermann et al., 2012) causing both washing out the platelet ice as well as mixing warm water into the water column associated with a thinning rate of the platelet-ice layer of approx. one meter per month from December onwards. The retreating fast ice also initializes the sea-ice break-up of the bay starting usually in December/January (Figure 2). The diminishing fast-ice zone causes the additional thinning of the platelet ice thickness (Figure 8 b) by, e.g., further washing out mechanisms. Even though the correlation between the change of fast-ice extent and the mean (maximum) platelet-ice accumulation between two consecutive surveys with a coefficient of 0.38 (0.35) is relatively low, Figure 8 shows that decreasing platelet-ice thicknesses are generally associated with retreating fast ice in Atka Bay. Also, Massom et al. (2018) has also shown that pack ice has a stabilizing effect as a buffer against ocean swells.

In contrast to the significant decreases in platelet-ice thickness beneath the fast ice in summer over the entire bay, the snow cover on top does not show a clear seasonal pattern but indicates a decrease in snow accumulation with increasing air temperature. However, even in summer, no consistent snow melting with associated strong mass loss is observed over the entire bay but strongest variability in snow depth over all sampling sites and all sampling years with a weak snow loss during summer months (Figure 6). This pattern is a result of both, temporary temperatures above freezing, which favor surface melting (Figure 8 a), and comparatively low wind speeds (Figure 3), preventing the accumulation of additional snow from the

https://doi.org/10.5194/tc-2019-293
Preprint. Discussion started: 9 January 2020
© Author(s) 2020. CC BY 4.0 License.

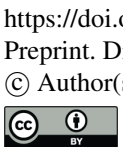

surrounding ice shelves. These results match watch well with results from studies on the seasonal cycle of snow properties in the inner pack ice zone of the Weddell Sea, as e.g. by Arndt et al. (2016), indicating the missing persistent summer melt from above.

Overall, the 9-years' time series for in-situ fast ice, snow and platelet ice thickness in Atka Bay does not show any trend over the analyzed study period, whereas their interannual variability is dominated by rather local effects as, e.g. icebergs, leading to a perennial fast-ice regime or small-scale strong snow accumulations (Figure 4). It is particularly remarkable that the mean annual platelet-ice accumulation rate of 4 meters (Table 1) is consistent with earlier investigations in the Atka Bay in end of the 1980s by Kipfstuhl (1991) suggesting a lack of trend in fast-ice properties and the adjacent ice shelfs even over the past decades.

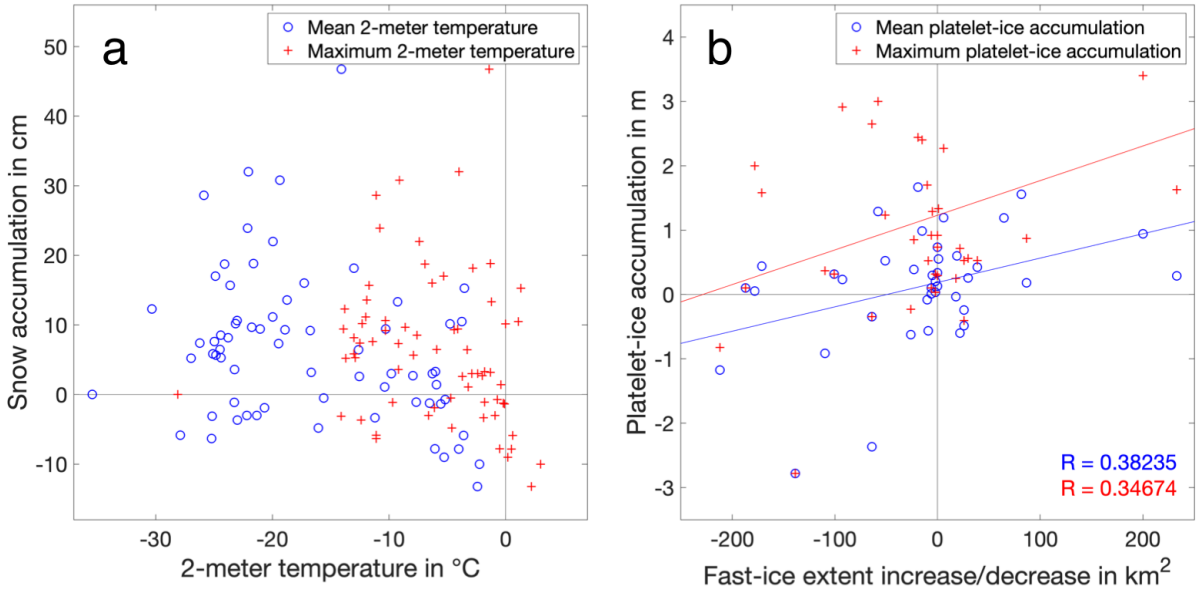

Figure 8: Correlation between (a) 2-meter air temperature (see Chapter 2.4) and the snow accumulation between two consecutive surveys, and (b) increasing (positive values) and decreasing (negative values) fast-ice extent and platelet-ice accumulation between two consecutive surveys. Blue circles and red crossed denote the respective mean and maximum values within the time frame between the consecutive measurements. Colored solid lines in Figure (b) show the linear regression between both parameters with the respective correlation coefficients R.

4.2 Spatial variability of fast-ice properties related to the distance to the ice-shelf edges

Investigating the spatial variability of the fast ice, its underlying platelet-ice layer and snow cover on top, when neglecting additional local disturbance factors, as, e.g. ice bergs, results clearly indicate differences between the evolution of platelet ice

https://doi.org/10.5194/tc-2019-293
Preprint. Discussion started: 9 January 2020
© Author(s) 2020. CC BY 4.0 License.


and snow as a function of the distance to the adjacent ice shelf edges in Atka Bay. In contrast, the fast ice does not show any spatial variability, but measures at the end of the season a nearly constant thickness of 2 meters across the bay both in west-east and south-north direction (Figure 7).

Analysis of the spatial distribution of platelet ice under the fast ice over the entire bay, on the standard transect, reveals that ATKA24 shows significantly less platelet ice than all other sampling sites. In contrast, the parallel transect towards the south indicates a significant local increase in platelet-ice accumulation at the closest sampling point to the eastern shelf ice edge (ATKA21p). Perpendicular sampling transects from close to the southern shelf ice edge towards the fast-ice edge in the north show a strong accumulation of platelet ice near the ice shelf edge followed by a moderate decrease in platelet ice thickness towards the north, which rapidly decreases about 5 kilometers off the fast-ice edge. This thickness gradient is much more pronounced on the south-north transect in the central area of the bay than to the west. Moreover, considering the entire time series of the west-east transect, the strongest platelet-ice accumulation is observed in the central area of the bay (ATKA07 and ATKA11). Summarizing all these observations, we hypothesize on the one hand that the strongest outflow of supercooled water and thus associated with platelet ice leads from the south centrally into the Atka Bay. On the other hand, local under-water topographic features of the ice shelf at the eastern edge of Atka Bay might lead to a blocking of oceanic circulation patterns and therefore the movement of platelet ice causing the large platelet-ice accumulation at ATKA21p and the low long-term observed accumulation rate north of it at ATKA24 (Figure 4). The strongly decreasing gradient in the platelet-ice thickness towards the sea-ice edge might be due to increasing distance from the source of the platelet ice under the ice shelf and related washout effects, since at the time of the measurement the pack ice in front of the bay was already broken open allowing for wind-induced currents and locally solar-heated water (so-called mode 3 incursions, Jacobs et al. (1992)) (Figure 1). Also, the fact that the northernmost sampling points are located at the edge of the bay or already outside of it, so that the predominant ocean current transporting warm Antarctic Surface Water towards the fast-ice area intensifying the effect (Hattermann et al., 2012; Hoppmann et al., 2015a).

From this, it can be generalized that relatively little platelet ice can accumulate under narrow fast-ice areas, since these are exposed to stronger oceanic currents and associated washout effects as well as warm water incursions. Comparative analyses to other study regions are not possible, since, to our knowledge, no comparable transects were carried out in other Antarctic fast-ice regions with platelet ice beneath.

In order to better understand day-to-day, seasonal and annual oscillations of oceanic currents and heat fluxes from the shelf ice to the fast-ice covered area and beyond, it is planned to install more autonomous measuring systems (buoys, Grosfeld et al. (2015)) on and under the sea ice. In addition, regular vertical ocean profiles (CTD) at certain sampling sites across the bay will complement the measurements.

Examining the spatial distribution of snow over the bay, the considerably lower snow depth at ATKA24 compared to all other sampling sites is striking. This anomaly is associated to the proximity to the surrounding ice shelf (approx. 1 km), which leads in the immediate vicinity to lee and thus to smaller snow thicknesses. Due to the prevailing easterly winds in the bay (Figure 3), an east-west gradient in snow thickness could have been expected over the rest of the bay. However, this gradient cannot

https://doi.org/10.5194/tc-2019-293
Preprint. Discussion started: 9 January 2020
© Author(s) 2020. CC BY 4.0 License.


be determined on average over the entire time series. This is due to temporary local disturbance factors in the bay, such as icebergs and pressure ridges, which additionally influence the snow distribution and thus lead to a comparatively homogeneous distribution of the snow thickness over the central part of Atka Bay. A south-north survey of the bay at the beginning of austral summer 2018 reveals a trend of decreasing snow depth towards the sea-ice edge in the north with a stronger gradient near the ice edge, commencing approx. 5 km off it (Figure 7), which is in line with the northern end of the shelf ice edge (Figure 1) and associated decreasing offshore winds and consequently less snow redistribution.

Due to the generally thick snow cover on Antarctic sea ice (Kern and Ozsoy-Çiçek, 2016; Markus and Cavalieri, 1998; Massom et al., 2001b), flooding of the snow/ice interface and the resulting formation of snow-ice is a widespread phenomenon in the Southern Ocean and contributes significantly to the sea-ice mass budget in the area (Eicken et al., 1995; Jeffries et al., 2001). While Günther and Dieckmann (1999) observed no flooding in Atka Bay during their study, Kipfstuhl (1991) reported flooding in relation to snow loads greater than 1 meter, an observation that we can largely confirm with our data. Exceptions are measurements on comparatively thin ice, that already showed a sufficient snow layer, e.g. in the austral winter 2010 and 2011 at ATKA21, leading to a negative freeboard and potential flooding already early in the season (Figure 5). Consequently, taking all conducted freeboard measurements on seasonal fast ice into account, 55 % of the data indicate a negative freeboard, i.e. potential flooding and associated snow-ice formation can be assumed. While the snow cover reduces the buoyancy of the sea ice and accelerates flooding, the underlying platelet ice counteracts this by adding additional buoyancy. However, neglecting the platelet-ice layer reduces the freeboard by 0.09 ± 0.06 m, but still a negative freeboard is derived in half of the calculations. Thus, the spatial distribution of the sign of the freeboard and therefore also the flooding of the snow/ice interface is essentially controlled by the snow layer on top of the fast ice in Atka Bay. The thickness of the underlying platelet-ice layer below in turn contributes to the resulting thickness of the flooded layer and consequently to the thickness of the expected snow-ice layer.

4.3 Impact of local disturbances on bay-wide properties and processes

The greatest local effect on the fast- ice conditions, the underlying plate ice and the snow on top of it are due to the icebergs at the edge of Atka Bay, as well as those that are enclosed by sea ice inside the bay in autumn, and thus stay there for the following year. Thus, the large iceberg B15G grounded in front of Atka Bay sheltering the fast ice in the bay and consequently preventing sea-ice break-up in the following summer (Hoppmann et al., 2015b) caused second-year fast ice in the bay in 2013. Our measurements have shown that this had hardly any effect on the monthly accumulation rates for snow and platelet ice, but rather that these were within the same range as in the years of seasonal sea-ice cover. Accordingly, for perennial sea ice, the total annual snow and platelet-ice thicknesses are approximately twice as thick as in the other years and average to 1.30 ± 0.60 m and 7.84 ± 1.33 m, respectively. Higher snow loads do also increase the probability and extent of flooding. This is not only observed for years of perennial sea ice but also for local disturbances due to small icebergs inside of the bay. In contrast, the perennial fast-ice thickness is not as linear: Due to the insulating snow cover on top and platelet ice layer underneath, as well

https://doi.org/10.5194/tc-2019-293
Preprint. Discussion started: 9 January 2020
© Author(s) 2020. CC BY 4.0 License.


as the already 2-meter seasonal thickness of it, steady thermodynamic growth does not play a role. Instead, dynamical growth as well as growth related to compaction of platelet ice layer dominates the thickening of the perennial fast ice, adding up to an average thickness of 4.19 ± 1.90 m, which is even more than double the thickness of seasonal sea ice in the bay. Thus, this multi-layered thick ice cover, separating the atmosphere from the ocean, is preventing the exchange of any fluxes between the two climate system components, and therefore also strongly influences the ice-associated ecosystem. From Günther and Dieckmann (1999) it is known that about 99% the total fast-ice biomass originates from algae being attached to the platelets that concealed to the fast-ice bottom. In contrast, the relatively thick snow layer on the fast ice in Atka Bay prevents a significant light input to the sea-ice bottom and thus additional biomass production. However, so far relatively little is known about the adaptation of the ecosystem in the upper ocean to perennial fast-ice conditions and the quantitative significance of, for example, small-scale and only temporary formation of openings in the ice (i.e. cracks and leads) have for the system. Also, future investigations on the effects of the rapidly increasing light level under the ice on the ecosystem within the platelet-ice layer due to the retreating pack-ice in front of the bay in spring would be of high interest to broaden and increase our knowledge on the connection between the physical and biological components of the eco- and climate system in one of the coastal key regions of Antarctica.

5 Conclusion

This study presents a semi-continuous record of fast-ice thickness, snow depth, freeboard, and sub-ice platelet layer thickness across Atka Bay from 2010 to 2018. Using this longest time series within AFIN, we can improve our understanding of the interactions between atmosphere, fast ice, ocean and ice shelf along with their seasonal and interannual variability in one of the key regions of Antarctica.

For the period of the study presented and beyond, considering individual measurements of 1980 and 1990, the predominantly seasonal character of the fast-ice regime in Atka Bay is evident without a noticeable trend for any of the analyzed variables. The absence of trend and seasonality of surface characteristics associated with the year-round snow cover and negligible surface melting coincides with the prevailing conditions in the Antarctic pack-ice zone. Hence, the described observations in Atka Bay over the last nine years allow not only to describe the initial conditions of sea ice/ocean/shelf ice interaction, but also to capture processes and properties of pack ice prior to possible future changes of pack ice in, e.g., the Weddell Sea, due to climate change.

Atka Bay is dominated by strong cyclonic events in the area causing easterly winds, which determine not only the freeze-up of the bay in autumn and breakup during summer months but also govern the year-round snow redistribution on the ice. The consequent substantial annual snow accumulation determines both the magnitude and duration of thermodynamical sea-ice growth as well as magnitude and spatial distribution of the frequent negative freeboard and related flooding of the snow/ice interface, and thus consequent snow-ice growth. In contrast, the annual thick layer of the buoyant platelet-ice under the fast ice contributes significantly to the sea-ice growth from below. However, our results indicate that although the platelet ice

https://doi.org/10.5194/tc-2019-293
Preprint. Discussion started: 9 January 2020
© Author(s) 2020. CC BY 4.0 License.


accretion partly offsets the negative freeboard, it cannot return the snow/ice interface above sea level again. We therefore suggest that the snow layer on top is the main driver controlling the energy and mass budgets of the fast ice in Atka Bay, and with that also the ice-associated ecosystem.

Considering the platelet ice layer in detail, we revealed that although the annual platelet ice accumulation of four meters is independent of annual or perennial fast ice, the seasonal and interannual variability of the layer and thus of the oceanic circulation patterns coming from the ice shelf is hardly understood. We therefore propose to extend the measurements in the bay spatially and to supplement them with additional regular oceanic measurements. This combination would allow to quantify the seasonal interactions between sea ice, ocean and shelf ice even more precisely and thus to better understand current patterns and accumulation rates of platelet ice and associated biomass under the ice as a function of the distance to the shelf-ice and sea- ice edge. These results would provide a solid basis to be applied to all fast-ice areas around Antarctica, and thus make a fundamental contribution to the understanding of the Antarctic climate system.

Data availability

All presented meteorological data are archived in PANGAEA at https://doi.pangaea.de/10.1594/PANGAEA.908826 . All fast-ice data are archived in PANGAEA at https://doi.pangaea.de/10.1594/PANGAEA.908860 .

Author contribution

MN is the principle investigator of the AFIN work at Neumayer Station III. SA conducted all analysis for the paper. HS contributed the meteorological data sets and respective analysis. AF contributed the fast-ice extent data set and respective analysis. SA wrote the paper and all co-authors contributed to the discussion and gave input for writing.

Competing interests

The authors declare that they have no conflict of interest.

Acknowledgements

We are most grateful to the overwintering teams at Neumayer Station III from 2010 to 2018 for their conducted measurements on the fast ice in Atka Bay. Special thanks are due to the respective meteorologists of the teams who led the sea ice work on site. Also, our work and research at Neumayer Station III would not have been possible without the extensive support of the AWI logistics. We also acknowledge the scientific support of Christian Haas, the logistical support of Anja Nicolaus, and the technical support of Jan Rohde, all from the Sea Ice Physics section at AWI. This work was supported by the German Research Council (DFG) in the framework of the priority programme ‘‘Antarctic Research with comparative investigations in Arctic

© Author(s) 2020. CC BY 4.0 License.


ice areas'' by grants to SPP1158, HE2740/12, NI1092/2 and AR1236/1, and the Alfred-Wegener-Institut Helmholtz-Zentrum für Polar- und Meeresforschung. This research was also supported under Australian Research Council's Special Research Initiative for Antarctic Gateway Partnership (Project ID SR140300001).

References

Aoki, S.: Breakup of land-fast sea ice in Lützow-Holm Bay, East Antarctica, and its teleconnection to tropical Pacific sea surface temperatures, Geophysical research letters, 44, 3219-3227, 2017.

Arndt, S., Willmes, S., Dierking, W., and Nicolaus, M.: Timing and regional patterns of snowmelt on Antarctic sea ice from passive microwave satellite observations, Journal of Geophysical Research - Oceans, 121, 5916-5930, 10.1002/2015JC011504, 2016.

Arndt, S., Asseng, J., Behrens, L. K., Hoppmann, M., Hunkeler, P. A., Ludewig, E., Müller, H., Paul, S., Rau, A., Schmidt, T., Schmithüsen, H., Schulz, H., Stautzebach, E., and Nicolaus, M.: Thickness and properties of sea ice and snow of land-fast sea ice in Atka Bay in 2010-2018, reference list of 9 datasets, Alfred Wegener Institute, Helmholtz Centre for Polar and Marine Research, Bremerhaven, PANGAEA, https://doi.pangaea.de/10.1594/PANGAEA.908860, 2019.

Dammann, D. O., Eriksson, L. E. B., Mahoney, A. R., Eicken, H., and Meyer, F. J.: Mapping pan-Arctic landfast sea ice stability using Sentinel-1 interferometry, The Cryosphere, 13, 557-577, 10.5194/tc-13-557-2019, 2019.

Divine, D., Korsnes, R., and Makshtas, A.: Variability and climate sensitivity of fast ice extent in the north-eastern Kara Sea, Polar Research, 22, 27-34, 10.1111/j.1751-8369.2003.tb00092.x, 2003.

Druckenmiller, M. L., Eicken, H., Johnson, M. A., Pringle, D. J., and Williams, C. C.: Toward an integrated coastal sea-ice observatory: System components and a case study at Barrow, Alaska, Cold Regions Science and Technology, 56, 61-72, 10.1016/j.coldregions.2008.12.003, 2009.

Eicken, H., and Lange, M. A.: Development and properties of sea ice in the coastal regime of the southeastern Weddell Sea, Journal of Geophysical Research: Oceans, 94, 8193-8206, 10.1029/JC094iC06p08193, 1989.

Eicken, H., Lange, M. A., Hubberten, H. W., and Wadhams, P.: Characteristics and distribution patterns of snow and meteoric ice in the Weddell Sea and their contribution to the mass balance of sea ice, Annales Geophysicae-Atmospheres Hydrospheres and Space Sciences, 12, 80-93, 10.1007/s00585-994-0080-x, 1994.

Eicken, H., Fischer, H., and Lemke, P.: Effects of the snow cover on Antarctic sea ice and potential modulation of its response to climate change, Annals of Glaciology, 21, 369-376, 10.3189/S0260305500016086, 1995.

Foldvik, A. a. K., T. : Thermohaline convection in the vicinity of an ice shelf, in: Polar oceans, Proceedings of the Polar Oceans Conference held at McGill University, Montreal, May, 1974, edited by: Dunbar, M. J., Arctic Institute of North America, Calgary, Alberta, 247-255, 1977.

Fraser, A. D., Massom, R. A., Michael, K. J., Galton-Fenzi, B. K., and Lieser, J. L.: East Antarctic landfast sea ice distribution and variability, 2000–08, Journal of Climate, 25, 1137-1156, 2012.

https://doi.org/10.5194/tc-2019-293
Preprint. Discussion started: 9 January 2020
© Author(s) 2020. CC BY 4.0 License.


Fraser, A. D., Ohshima, K. I., Nihashi, S., Massom, R. A., Tamura, T., Nakata, K., Williams, G. D., Carpentier, S., and Willmes, S.: Landfast ice controls on sea-ice production in the Cape Darnley Polynya: A case study, Remote Sensing of Environment, 233, 111315, 2019.

Galley, R. J., Else, B. G. T., Howell, S. E. L., Lukovich, J. V., and Barber, D. G.: Landfast Sea Ice Conditions in the Canadian Arctic: 1983-2009, Arctic, 65, 133-144, 2012.

Giles, A. B., Massom, R. A., and Lytle, V. I.: Fast-ice distribution in East Antarctica during 1997 and 1999 determined using RADARSAT data, Journal of Geophysical Research: Oceans, 113, 2008.

Gough, A. J., Mahoney, A. R., Langhorne, P. J., Williams, M. J. M., Robinson, N. J., and Haskell, T. G.: Signatures of supercooling: McMurdo Sound platelet ice, Journal of Glaciology, 58, 38-50, Doi 10.3189/2012jog10j218, 2012.

Grosfeld, K., Treffeisen, R., Asseng, J., Bartsch, A., Bräuer, B., Fritzsch, B., Gerdes, R., Hendricks, S., Hiller, W., and Heygster, G.: Online sea-ice knowledge and data platform < www. meereisportal. de >, Polarforschung, 85, 143-155, 2015.

Günther, S., and Dieckmann, G. S.: Seasonal development of algal biomass in snow-covered fast ice and the underlying platelet layer in the Weddell Sea, Antarctica, Antarct Sci, 11, 305-315, 1999.

Haas, C.: The seasonal cycle of ERS scatterometer signatures over perennial Antarctic sea ice and associated surface ice properties and processes, Ann Glaciol, 33, 69-73, 10.3189/172756401781818301, 2001.

Haas, C., Thomas, D. N., and Bareiss, J.: Surface properties and processes of perennial Antarctic sea ice in summer, Journal of Glaciology, 47, 613-625, 10.3189/172756501781831864, 2001.

Hattermann, T., Nøst, O. A., Lilly, J. M., and Smedsrud, L. H.: Two years of oceanic observations below the Fimbul Ice Shelf, Antarctica, Geophysical Research Letters, 39, 2012.

Heil, P.: Atmospheric conditions and fast ice at Davis, East Antarctica: A case study, Journal of Geophysical Research: Oceans, 111, 2006.

Heil, P., Gerland, S., and Granskog, M.: An Antarctic monitoring initiative for fast ice and comparison with the Arctic, The Cryosphere Discussions, 5, 2437-2463, 2011.

Hoppmann, M., Nicolaus, M., Hunkeler, P. A., Heil, P., Behrens, L. K., Konig-Langlo, G., and Gerdes, R.: Seasonal evolution of an ice-shelf influenced fast-ice regime, derived from an autonomous thermistor chain, Journal of Geophysical Research-Oceans, 120, 1703-1724, 10.1002/2014jc010327, 2015a.

Hoppmann, M., Nicolaus, M., Paul, S., Hunkeler, P. A., Heinemann, G., Willmes, S., Timmermann, R., Boebel, O., Schmidt, T., Kuhnel, M., Konig-Langlo, G., and Gerdes, R.: Ice platelets below Weddell Sea landfast sea ice, Annals of Glaciology, 56, 175-190, 10.3189/2015AoG69A678, 2015b.

Hunkeler, P. A., Hoppmann, M., Hendricks, S., Kalscheuer, T., and Gerdes, R.: A glimpse beneath Antarctic sea ice: Platelet layer volume from multifrequency electromagnetic induction sounding, Geophysical Research Letters, 43, 222-231, 2016.

Jacobs, S., Helmer, H., Doake, C., Jenkins, A., and Frolich, R.: Melting of ice shelves and the mass balance of Antarctica, Journal of Glaciology, 38, 375-387, 1992.

JCOMM Expert Team on Sea Ice: WMO Sea-Ice Nomenclature I-III, 2015.

© Author(s) 2020. CC BY 4.0 License.


Jeffries, M., Li, S., Jana, R., Krouse, H., and Hurst-Cushing, B.: Late winter first-year ice floe thickness variability, seawater flooding and snow ice formation in the Amundsen and Ross Seas, Antarctic Sea Ice: Physical processes, interactions and variability, 74, 69-87, 1998.

Jeffries, M. O., Krouse, H. R., Hurst-Cushing, B., and Maksym, T.: Snow-ice accretion and snow-cover depletion on Antarctic first-year sea-ice floes, Annals of Glaciology, 33, 51-60, 2001.

Kawamura, T., Jeffries, M. O., Tison, J.-L., and Krouse, H. R.: Superimposed-ice formation in summer on Ross Sea pack-ice floes, Annals of glaciology, 39, 563-568, 2004.

Kern, S., and Ozsoy-Çiçek, B.: Satellite Remote Sensing of Snow Depth on Antarctic Sea Ice: An Inter-Comparison of Two Empirical Approaches, Remote Sensing, 8, 450, 10.3390/rs8060450, 2016.

Kipfstuhl, J.: Zur Entstehung von Unterwassereis und das Wachstum und die Energiebilanz des Meereises in der Atka Bucht, Antarktis= On the formation of underwater ice and the growth and energy budget of the sea ice in Atka Bay, Antarctica, Berichte zur Polarforschung (Reports on Polar Research), 85, 1991.

König-Langlo, G., and Loose, B.: The Meteorological Observatory at Neumayer Stations (GvN and NM-II) Antarctica, Berichte zur Polar-und Meeresforschung (Reports on Polar and Marine Research), 76, 25-38, 2007.

Kwok, R., Pang, S. S., and Kacimi, S.: Sea ice drift in the Southern Ocean: Regional patterns, variability, and trends, Elem Sci Anth, 5, 2017.

Langhorne, P. J., Hughes, K. G., Gough, A. J., Smith, I. J., Williams, M. J. M., Robinson, N. J., Stevens, C. L., Rack, W., Price, D., Leonard, G. H., Mahoney, A. R., Haas, C., and Haskell, T. G.: Observed platelet ice distributions in Antarctic sea ice: An index for ocean-ice shelf heat flux, Geophysical Research Letters, 42, 5442-5451, 10.1002/2015gl064508, 2015.

Lemieux, J. F., Dupont, F., Blain, P., Roy, F., Smith, G. C., and Flato, G. M.: Improving the simulation of landfast ice by combining tensile strength and a parameterization for grounded ridges, Journal of Geophysical Research: Oceans, 121, 7354-7368, 2016.

Li, L., and Pomeroy, J. W.: Estimates of threshold wind speeds for snow transport using meteorological data, J Appl Meteorol, 36, 205-213, 10.1175/1520-0450, 1997.

Mahoney, A., Eicken, H., Gaylord, A. G., and Shapiro, L.: Alaska landfast sea ice: Links with bathymetry and atmospheric circulation, Journal of Geophysical Research: Oceans, 112, 2007a.

Mahoney, A., Eicken, H., and Shapiro, L.: How fast is landfast sea ice? A study of the attachment and detachment of nearshore ice at Barrow, Alaska, Cold Regions Science and Technology, 47, 233-255, 10.1016/j.coldregions.2006.09.005, 2007b.

Mahoney, A. R., Eicken, H., Gaylord, A. G., and Gens, R.: Landfast sea ice extent in the Chukchi and Beaufort Seas: The annual cycle and decadal variability, Cold Regions Science and Technology, 103, 41-56, https://doi.org/10.1016/j.coldregions.2014.03.003, 2014.

Markus, T., and Cavalieri, D. J.: Snow depth distribution over sea ice in the Southern Ocean from satellite passive microwave data, Antarctic sea ice: physical processes, interactions and variability, 19-39, 1998.

Massom, R., Hill, K., Lytle, V., Worby, A., Paget, M., and Allison, I.: Effects of regional fast-ice and iceberg distributions on the behaviour of the Mertz Glacier polynya, East Antarctica, Annals of Glaciology, 33, 391-398, 2001a.

https://doi.org/10.5194/tc-2019-293
Preprint. Discussion started: 9 January 2020
© Author(s) 2020. CC BY 4.0 License.


Massom, R., Jacka, K., Pook, M., Fowler, C., Adams, N., and Bindoff, N.: An anomalous late-season change in the regional sea ice regime in the vicinity of the Mertz Glacier Polynya, East Antarctica, Journal of Geophysical Research: Oceans, 108, 2003.

Massom, R. A., Eicken, H., Haas, C., Jeffries, M. O., Drinkwater, M. R., Sturm, M., Worby, A. P., Wu, X. R., Lytle, V. I., Ushio, S., Morris, K., Reid, P. A., Warren, S. G., and Allison, I.: Snow on Antarctic Sea ice, Rev Geophys, 39, 413-445, 10.1029/2000rg000085, 2001b.

Massom, R. A., Hill, K., Barbraud, C., Adams, N., Ancel, A., Emmerson, L., and Pook, M. J.: Fast ice distribution in Adélie Land, East Antarctica: interannual variability and implications for emperor penguins Aptenodytes forsteri, Marine Ecology Progress Series, 374, 243-257, 2009.

Massom, R. A., Giles, A. B., Fricker, H. A., Warner, R. C., Legrésy, B., Hyland, G., Young, N., and Fraser, A. D.: Examining the interaction between multi-year landfast sea ice and the Mertz Glacier Tongue, East Antarctica: Another factor in ice sheet stability?, Journal of Geophysical Research: Oceans, 115, 2010.

Massom, R. A., Scambos, T. A., Bennetts, L. G., Reid, P., Squire, V. A., and Stammerjohn, S. E.: Antarctic ice shelf disintegration triggered by sea ice loss and ocean swell, Nature, 558, 383-389, 10.1038/s41586-018-0212-1, 2018.

Murphy, E. J., Clarke, A., Symon, C., and Priddle, J.: Temporal variation in Antarctic sea-ice: analysis of a long term fast-ice record from the South Orkney Islands, Deep Sea Research Part I: Oceanographic Research Papers, 42, 1045-1062, 1995.

Nicolaus, M., and Grosfeld, K.: Ice-Ocean Interactions underneath the Antarctic Ice Shelf Ekströmisen, Polarforschung, 72, 17-29, 2004.

Olason, E.: A dynamical model of Kara Sea land-fast ice, Journal of Geophysical Research-Oceans, 121, 3141-3158, 10.1002/2016JC011638, 2016.

Polyakov, I. V., Alekseev, G. V., Bekryaev, R. V., Bhatt, U. S., Colony, R., Johnson, M. A., Karklin, V. P., Walsh, D., and Yulin, A. V.: Long-Term Ice Variability in Arctic Marginal Seas, Journal of Climate, 16, 2078-2085, 10.1175/1520-0442(2003)016<2078:LIVIAM>2.0.CO;2, 2003.

Schmithüsen, H., König-Langlo, G., Müller, H., and Schulz, H.: Continuous meteorological observations at Neumayer station (2010-2018),reference list of 108 datasets, Alfred Wegener Institute, Helmholtz Centre for Polar and Marine Research, Bremerhaven, PANGAEA, https://doi.pangaea.de/10.1594/PANGAEA.908826, 2019.

Selyuzhenok, V., Krumpen, T., Mahoney, A., Janout, M., and Gerdes, R.: Seasonal and interannual variability of fast ice extent in the southeastern Laptev Sea between 1999 and 2013, Journal of Geophysical Research: Oceans, n/a-n/a, 10.1002/2015JC011135, 2015.

Selyuzhenok, V., Mahoney, A., Krumpen, T., Castellani, G., and Gerdes, R.: Mechanisms of fast-ice development in the south-eastern Laptev Sea: a case study for winter of 2007/08 and 2009/10, Polar Research, 36, Artn 1411140 10.1080/17518369.2017.1411140, 2017.

Smith, I. J., Langhorne, P. J., Haskell, T. G., Trodahl, H. J., Frew, R., and Vennell, M. R.: Platelet ice and the land-fast sea ice of McMurdo Sound, Antarctica, Annals of Glaciology, 33, 21-27, 2001.

Tamura, T., Williams, G., Fraser, A., and Ohshima, K.: Potential regime shift in decreased sea ice production after the Mertz Glacier calving, Nature communications, 3, 826, 2012.

https://doi.org/10.5194/tc-2019-293
Preprint. Discussion started: 9 January 2020
© Author(s) 2020. CC BY 4.0 License.


Tamura, T., Ohshima, K. I., Fraser, A. D., and Williams, G. D.: Sea ice production variability in Antarctic coastal polynyas, Journal of Geophysical Research: Oceans, 121, 2967-2979, 2016.

Williams, G., Bindoff, N., Marsland, S., and Rintoul, S.: Formation and export of dense shelf water from the Adélie Depression, East Antarctica, Journal of Geophysical Research: Oceans, 113, 2008.

Yu, Y., Stern, H., Fowler, C., Fetterer, F., and Maslanik, J.: Interannual Variability of Arctic Landfast Ice between 1976 and 2007, Journal of Climate, 27, 227-243, 10.1175/jcli-d-13-00178.1, 2014.